Conformational Dynamics of DNA Polymerase Probed with a Novel Fluorescent DNA Base Analogue[†]

Gudrun Stengel,[‡] Joshua P. Gill,[‡] Peter Sandin,[§] L. Marcus Wilhelmsson,[§] Bo Albinsson,[§] Bengt Nordén,[§] and David Millar*,[‡]

Department of Molecular Biology, The Scripps Research Institute, La Jolla, California 92037, and Department of Chemical and Biological Engineering/Physical Chemistry, Chalmers University of Technology, Gothenberg, Sweden

Received April 20, 2007; Revised Manuscript Received August 10, 2007

ABSTRACT: DNA polymerases discriminate between correct and incorrect nucleotide substrates during a "nonchemical" step that precedes phosphodiester bond formation in the enzymatic cycle of nucleotide incorporation. Despite the importance of this process in polymerase fidelity, the precise nature of the molecular events involved remains unknown. Here we report a fluorescence resonance energy transfer (FRET) system that monitors conformational changes of a polymerase−DNA complex during selection and binding of nucleotide substrates. This system utilizes the fluorescent base analogue 1,3-diaza-2-oxophenothiazine (tC) as the FRET donor and Alexa-555 (A555) as the acceptor. The tC donor was incorporated within a model DNA primer/template in place of a normal base, adjacent to the primer 3′ terminus, while the A555 acceptor was attached to an engineered cysteine residue (C751) located in the fingers subdomain of the Klenow fragment (KF) polymerase. The FRET efficiency increased significantly following binding of a correct nucleotide substrate to the KF−DNA complex, showing that the fingers had closed over the active site. Fluorescence anisotropy titrations utilizing tC as a reporter indicated that the DNA was more tightly bound by the polymerase under these conditions, consistent with the formation of a closed ternary complex. The rate of the nucleotide-induced conformational transition, measured in stopped-flow FRET experiments, closely matched the rate of correct nucleotide incorporation, measured in rapid quench-flow experiments, indicating that the conformational change was the rate-limiting step in the overall cycle of nucleotide incorporation for the labeled KF−DNA system. Taken together, these results indicate that the FRET system can be used to probe enzyme conformational changes that are linked to the biochemical function of DNA polymerase.

DNA polymerases are essential enzymes required by all living organisms to perform DNA replication and repair activities. All members of this large and diverse enzyme family perform the same basic function, catalyzing the template-directed addition of nucleoside monophosphate units onto the 3′ end of a nascent DNA primer strand (*1*). Despite their common enzymatic activity, DNA polymerases differ vastly in size, cellular roles, and replication fidelities. From amino acid sequence comparisons, DNA polymerases can be organized into seven families: A, B, C, D, X, Y, and RT (*2*, *3*). Structural studies of DNA polymerases from several of these families have revealed a common three-dimensional architecture of the polymerase domain, composed of fingers, palm, and thumb subdomains arranged in the form of a half-open right hand (*4*−*14*).

Pre-steady-state chemical kinetic studies of the A-family polymerases Klenow fragment (KF, *15*) and T7 DNA polymerase (*16*) have established that the polymerase activity of these enzymes occurs through the following sequence of events: (1) Initial binding of a DNA_n substrate (where *n* denotes the length of the primer strand) to the polymerase, forming a binary polymerase−DNA complex; (2) binding of a nucleotide substrate to form a ternary polymerase−DNA−dNTP complex; (3) isomerization of the ternary complex from an "inactive" to an "active" form; (4) the chemical step of phosphoryl transfer, during which the 3′ hydroxyl of the primer DNA attacks the α-phosphate of the incoming nucleotide according to a two-metal-ion catalytic mechanism (*17*); (5) a second isomerization step, presumably back to the inactive form; (6) pyrophosphate release; and (7) release or translocation of the DNA_{n+1} product. Similar kinetic studies have since established that DNA polymerases from families B (*18*), X (*19*), and Y (*20*−*22*) also function according to this scheme, although the rates of the elementary steps can vary widely. This multistep process allows the polymerase to discriminate between correct and incorrect nucleotide substrates at various points in the nucleotide incorporation cycle, thereby enhancing the overall fidelity. The initial nucleotide-binding step generally favors the correct nucleotide substrate, whereas the subsequent isomerization step is strongly inhibited by an incorrect nucleotide (*23*).

[†] Supported by the U.S. National Institutes of Health (Grant GM44060 to D.M.) and the Swedish Foundation for Strategic Research (senior individual grant to B.N.).

* Author to whom correspondence should be addressed: Department of Molecular Biology, The Scripps Research Institute, 10550 N. Torrey Pines Rd., La Jolla, CA 92037; tel (858) 784-9870; fax (858) 784-9067; e-mail millar@scripps.edu.

[‡] The Scripps Research Institute.

[§] Chalmers University of Technology.

10.1021/bi700755m CCC: $37.00
Published on Web 10/04/2007

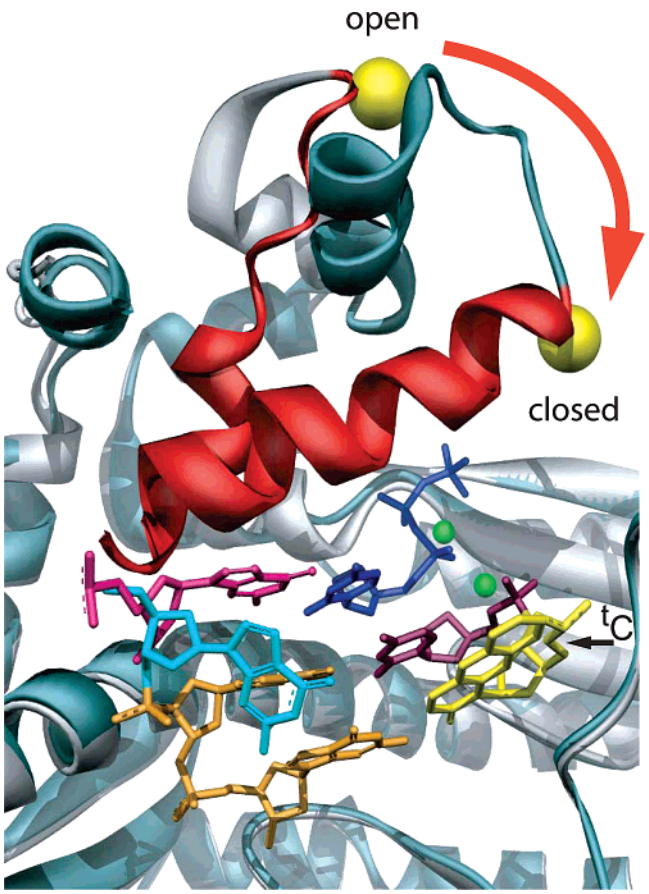

FIGURE 1: Closeup view of the catalytic center of the KF homologue Klentaq1 polymerase. Shown are overlaid crystal structures of the open binary (light gray ribbon) and closed ternary (dark green ribbon) complexes of Klentaq1 (ref *24*; PDB accession codes 2KTQ and 3KTQ, respectively). The O-helix is shown in red, highlighting the different positions of this helix in the open (upper) and closed (lower) conformations. The yellow balls correspond to the labeling position 751 of KF in the open and closed forms. The bound DNA is displayed in orange stick representation. The tC base used as a FRET donor in this study is highlighted in yellow and is modeled into the structure in place of the cytosine in the crystal structure. The base at the primer terminus is in purple, and the incoming nucleotide is in blue. The base in magenta corresponds to the templating base in the closed form, while the base in light blue represents the orientation of the templating base in the open form. The two divalent metal ions at the active site are shown as green spheres.

The nature of the nonchemical step preceding phosphoryl transfer is a question of significant interest in DNA polymerase enzymology, owing to the importance of this process in nucleotide selection and polymerase fidelity. However, the precise nature of the molecular events involved is still obscure, although several hypotheses have been advanced. Cocrystal structures of DNA polymerases in complex with DNA and nucleotide substrates have revealed two possible conformations of the fingers subdomain, termed "open" and "closed" (*24*−*26*). The main characteristics of the closed form are a tilt of the O-helix toward the DNA and alignment of the templating base with the incoming nucleotide (Figure 1). Since only the closed ternary complex has an appropriate alignment of all participating groups necessary to catalyze the phosphoryl transfer reaction, it was proposed that the prechemical step corresponds to an open-to-closed transition of the fingers (*24*). However, the results of molecular dynamics simulations of DNA polymerase β suggest that

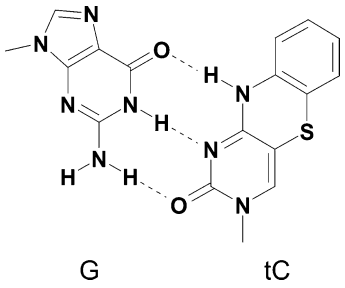

FIGURE 2: Chemical structure of G-tC base pair.

the prechemical step involves the rearrangement of critical amino acid residues within the active site (*27*). Alternatively, rapid kinetic studies of DNA polymerase β suggest that the prechemical step corresponds to the binding of a catalytic metal ion at the polymerase active site (*28*).

In view of the uncertainty surrounding the nature of the prechemical step during nucleotide incorporation, it is important to have methods that are capable of detecting conformational changes of a polymerase−DNA−dNTP ternary complex. We sought to develop a fluorescence resonance energy transfer (FRET)[1] system to monitor large-scale motions of a polymerase−DNA complex in solution. A key feature of the design concept is the use of the novel fluorescent base analogue 1,3-diaza-2-oxophenothiazine (tC) as the FRET donor. This tricyclic analogue of cytidine can form a normal Watson−Crick base pair with guanine (Figure 2) and can be accommodated within a DNA duplex without significant distortion of the normal B-form geometry or enhanced motional dynamics (*29*, *30*). Hence, a tC donor will adopt a well-defined position within a polymerase−DNA complex, which should help to simplify the interpretation of donor−acceptor distances obtained from FRET measurements. Most importantly, in contrast to many other known fluorescent base analogues, which are highly quenched when incorporated in DNA (*31*−*36*), the tC base retains a relatively high quantum yield and a long fluorescence lifetime in DNA (*37*). Hence, tC will serve as an efficient FRET donor suitable for long-range distance measurements, while the polarization anisotropy of the tC emission should be sensitive to binding events that lead to slow rotational diffusion of the labeled DNA.

In this study, we investigate the ability of the tC base analogue to serve as a reporter of polymerase−DNA interactions and conformational dynamics, in both FRET and anisotropy experiments. We first show that tC is tolerated by KF at critical positions within a DNA primer/template. We then construct a FRET system in which tC is used as a donor and a complementary A555 acceptor is attached to an engineered cysteine residue within the fingers subdomain of KF. This system is used to detect conformational changes of the polymerase−DNA complex induced upon binding of a correct nucleotide substrate, in both equilibrium and stopped-flow kinetic experiments. We have also measured the rate of nucleotide incorporation under the same conditions

[1] Abbreviations: tC, 1,3-diaza-2-oxophenothiazine; A555, Alexa-555; 2AP, 2-aminopurine; KF, Klenow fragment of *Escherichia coli* DNA polymerase I; FRET, fluorescence resonance energy transfer; MALDI-TOF, matrix-assisted laser desorption ionization time-of-flight; DTT, dithiothreitol; EDTA, ethylenediaminetetraacetic acid; BSA, bovine serum albumin.

as the stopped-flow FRET experiments. In addition, we also develop a fluorescence anisotropy system to quantify the thermodynamic stability of the polymerase−DNA complex, in the presence and absence of nucleotide substrates. Taken together, our results reveal new information about the nature and time scale of enzyme conformational changes during nucleotide selection and binding by KF.

EXPERIMENTAL PROCEDURES

Purification and Labeling of a Mutant Klenow Fragment Derivative. A plasmid encoding the D424A/C907S/S751C KF mutant was generously provided by Dr. Catherine Joyce (Yale University). A second plasmid encoding the D424A/C907S KF mutant was generated by use of the QuickChange kit (Stratagene). In both cases, the complete KF gene was sequenced to confirm the presence of the desired mutations. Expression and purification of KF mutants was carried out as described (*38*). The molecular weight of the KF mutants was verified by SDS−PAGE and MALDI-TOF spectrometry. Protein concentrations were determined spectrophotometrically at 280 nm with an ϵ_{280} value of 5.88×10^4 M^{-1} cm^{-1} for KF.

Acceptor-labeled KF was prepared by chemical coupling of Alexa-555 maleimide (Invitrogen, Carlsbad, CA) to the introduced cysteine residue of the C907S/S751C/D424A KF mutant. Typically 100 nmol of KF was reacted with a 3−5-fold molar excess of Alexa-555 maleimide in 50 mM phosphate buffer, pH 7.0, for at least 1 h at room temperature. The remaining excess free dye was removed by use of a Sephadex-G25 gel-filtration column equilibrated with 50 mM phosphate buffer, pH 7.5, and 1.7 M $(NH_4)_2SO_4$. The labeled protein was separated from unlabeled protein by hydrophobic interaction chromatography on a fast protein liquid chromatography (FPLC) system (Äkta, Amersham Pharmacia) equipped with a Resource ISO column (Amersham Pharmacia). The degree of labeling was determined from the dye and protein absorbances at 555 and 280 nm, respectivelywith the significant dye absorbance at 280 nm taken into account. The degree of labeling was typically 100% after FPLC purification. The protein was stored in 50 mM Tris-HCl, pH 7.5, and 1 mM EDTA at −80 °C.

Oligonucleotides. Primer (11-mer) and template (16-mer) oligo(deoxyribo)nucleotides were synthesized on a Gene Assembler (Pharmacia) by standard β-cyanoethyl phosphoramidite chemistry. Phosphoramidite derivatives of the normal DNA bases were purchased from Glen Research. 3-(2-Deoxy-β-D-ribofuranosyl)-1,3-diaza-2-oxophenothiazine was synthesized according to the procedure described (*35*) and converted to the 3′-*O*-phosphoramidite. The primer oligonucleotides used for fluorescence measurements contained 2′,3′-dideoxycytidine at the 3′ terminus to prevent nucleotide incorporation upon mixing with KF and nucleotide substrates. All oligonucleotides were purified by denaturing electrophoresis in 20% (w/v) polyacrylamide gels. Concentrations of the oligonucleotides were determined by measuring the UV absorption at 260 nm. The 260 nm extinction coefficients of the oligonucleotides were approximated by linear combination of the extinction coefficients of the natural nucleotides ($\epsilon_A = 15\,300$ M^{-1} cm^{-1}, $\epsilon_G = 11\,800$ M^{-1} cm^{-1}, $\epsilon_C = 7400$ M^{-1} cm^{-1}, $\epsilon_T = 9300$ M^{-1} cm^{-1}) and of the potassium salt of 1,3-diaza-2-oxophenothiazin-3-yl acetic acid ($\epsilon = 13\,500$ M^{-1} cm^{-1}) (*37*). To estimate the extinction coefficients of single-stranded oligomers, the linear combination of component nucleotide absorbances was multiplied by 0.9 to account for base stacking interactions. Primer/template duplexes were prepared by hybridizing the primer and template oligonucleotides at a 1:1.2 ratio in 50 mM Tris-HCl, pH 7.5, and 1 mM EDTA.

Primer Extension Assays. Reactions were initiated by adding 30 nM D424A/C907S KF to a solution of 400 nM primer/template duplex, and 200 μM of the particular dNTP. The reaction buffer contained 50 mM Tris-HCl, pH 7.5, 5 mM $MgCl_2$, 1 mM DTT, and 10% (v/v) glycerol. The reaction was stopped after 2 min by quenching 10 μL of the solution with 10 μL of 80% formamide (containing 50 mM EDTA). The extension products were separated on a 20% polyacrylamide denaturing gel (8 M urea, 1× TBE) and visualized by staining with SYBRgold (Invitrogen, Carlsbad, CA).

Steady-State FRET Measurements. All emission spectra were recorded on a SLM Aminco 8100 spectrofluorometer at a temperature of 20 °C. The tC donor was excited at 393 nm, and the emission spectrum of the donor and A555 acceptor was collected under magic-angle conditions (8 nm slits for excitation and emission). Binary complexes were formed by addition of 1 μM A555-KF to 500 nM primer/template. Ternary complexes additionally contained 1 mM of the chosen dNTP. The assay buffer was 50 mM Tris-HCl, pH 7.5, 5 mM $MgCl_2$, 1 mM DTT, 10% (v/v) glycerol, and 0.5 mg/mL BSA. The FRET efficiency, E, was calculated according to $E = 1 - (I_{DA}/I_D)$, where I_{DA} is the donor emission intensity of the D/A complex (binary complex of P1/T1 and A555-labeled KF or ternary complex of P1/T1, A555-KF, and dNTP) and I_D is the emission intensity of the corresponding donor-only complex (binary complex of duplex P1/T1 and unlabeled KF or ternary complex of P1/T1, unlabeled KF, and dNTP). The donor−acceptor distance, R, was calculated according to $R = R_0(E^{-1} - 1)^{1/6}$, where R_0 is the Förster distance. The Förster distance was evaluated according to the standard method (*39*).

Fluorescence Anisotropy Titrations. The fluorescence anisotropy of tC, r, was measured by use of L-format geometry ($\lambda_{em} = 505$ nm) and calculated as $r = (I_{vv} - GI_{vh})/(I_{vv} + 2GI_{vh})$, where I is the polarized fluorescence intensity and the first and second letters of the subscript denote the orientation (either vertical, v, or horizontal, h) of the excitation and emission polarizers, respectively. The grating correction factor G accounts for the differential transmission efficiency of vertically and horizontally polarized emission through the emission monochromator and was separately determined prior to each measurement. Fluorescence anisotropy titrations started with 100 nM primer/template alone or plus 1 mM dATP (correct nucleotide) or 1 mM dCTP (incorrect nucleotide). Unlabeled D424A/C907S/S751C mutant KF was added in gradually increasing amounts until a constant tC anisotropy level was reached. The resulting titration profiles were fitted with a quadratic equation describing a 1:1 association model (*40*) in order to determine the apparent dissociation constant (K_d) for the DNA−protein complex.

Stopped-Flow FRET Measurements. Kinetic measurements were performed in a stopped-flow mixing cell attached to the SLM Aminco 8100 fluorometer (mixing dead time

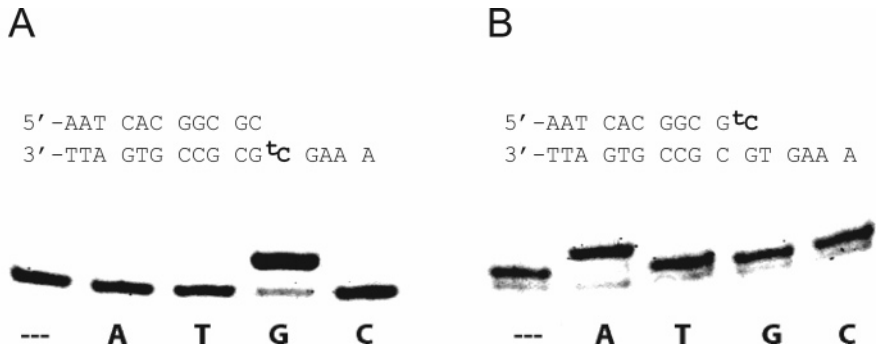

FIGURE 3: Single nucleotide primer extension reactions with primer/templates containing the base analogue tC (denoted by tC). (A) The tC base at the templating position specifically directs the incorporation of dGTP. (B) Presence of tC at the 3′ end of the primer strand does not perturb the ability of the polymerase to incorporate the correct nucleotide dATP opposite template T. Reaction mixtures contained 30 nM D424A/C907S mutant KF, 400 nM primer/template duplex, and 200 μM of the particular dNTP in a buffer of 50 mM Tris-HCl, pH 7.5, 5 mM $MgCl_2$, 1 mM DTT, and 10% (v/v) glycerol. The reaction was quenched after 2 min with a solution of 80% formamide containing 50 mM EDTA; the extension products were separated on a 20% polyacrylamide denaturing gel and visualized by staining with SYBRgold.

$\sim$ 3 ms). The reaction buffer, 50 mM Tris/HCl, pH 7.5, 5 mM $MgCl_2$, 1 mM DTT, 10% (v/v) glycerol, and 0.5 mg/mL BSA, was degassed before the experiments. A solution of preformed binary complex (1 μM A555-KF and 500 nM primer/template) was rapidly mixed with a 1 mM solution of the particular dNTP. All concentrations are final concentrations after mixing. The tC donor was excited at 393 nm (4 nm slits for observation of the acceptor, 8 nm slits for observation of the donor). The change of tC emission over time was observed by use of a 530 nm bandpass filter ($\pm$20 nm) and the A555 emission was collected through a 550 nm long pass cutoff filter. The integration time was 4 ms, yielding a time resolution of 5 ms. All measurements were performed at a temperature of 20 °C. The donor and acceptor emission transients were fitted with a single-exponential function to obtain the corresponding rates of the nucleotide-induced conformational transition.

Rapid Quench-Flow Measurements of Nucleotide Incorporation. The rate of single nucleotide incorporation reactions was measured under pre-steady-state conditions on a Kintek RQF3 rapid quench-flow instrument. Reactions were initiated by mixing 0.5 mM dATP with a preformed binary polymerase−DNA complex, containing 300 nM A555-labeled KF and 200 nM extendable P1/T1 duplex. The P1 primer oligonucleotide was radiolabeled at the 5′ end with ^{32}P. All concentrations are final concentrations after mixing. The reaction buffer was 50 mM Tris/HCl, pH 7.5, 5 mM $MgCl_2$, 1 mM DTT, 10% (v/v) glycerol, and 0.5 mg/mL BSA. The reaction was quenched with 0.5 M EDTA solution at times ranging from 4 ms to 8 s. All reactions were performed at 20 °C. The single nucleotide extension products were separated on a DNA sequencing gel (15% polyacrylamide, 8 M urea, and 1$\times$ TBE) and visualized on a phosphorimager (Molecular Dynamics). The relative intensities of the extended and unextended primer bands were quantified with ImageQuant software (Molecular Dynamics). The reaction time course data were fitted with the equation $C_{+1}(t) = A(1 - e^{-k_{pol}t})$, where $C_{+1}(t)$ is the concentration of the extended primer generated after reaction time t and k_{pol} is the rate of polymerase activity. Similar reactions were performed with unlabeled KF and/or an unlabeled primer/template P1/T1 (tC replaced by C).

5′-AAT CAC GGC tCC$_{dd}$ (P1)
3′-TTA GTG CCG GGT GAA A (T1)

FIGURE 4: Base sequence of the primer/template used for steady-state and stopped-flow FRET studies. The tC base is denoted tC and shown in boldface type. The dd designation at the 3′ end of the primer strand indicates that the terminal nucleotide contains a 2′,3′-dideoxy modification.

RESULTS

Recognition of tC by Klenow Fragment. While tC has the potential to form a normal Watson−Crick base pair with guanine (Figure 2), the recognition properties of tC within the confines of the active-site environment of a DNA polymerase are unknown. Consequently, we created an 11/16-mer primer/template with tC located at the templating position and then tested the ability of each of the four natural deoxynucleoside triphosphates to be incorporated by KF during a single round of primer extension (Figure 3A). Notably, the primer strand was extended only in the presence of dGTP as a nucleotide substrate, indicating that the expected tC-G base pair is formed within the polymerase active site and that the selectivity of KF for incorporation of a complementary nucleotide is preserved even when the enzyme encounters an unnatural templating base. We also carried out single nucleotide incorporation reactions with a primer/template containing tC at the 3′ end of the primer strand and a normal thymine base at the templating position. In this case, the incoming nucleotide becomes covalently linked to the terminal tC group. As expected, extension was observed only when the correct nucleotide dATP was added to the reaction mixture (Figure 3B), indicating that the presence of tC at the primer terminus does not compromise the ability of KF to recognize and incorporate the correct nucleotide substrate. Taken together, these results confirm that tC is well tolerated at critical positions within the primer/template.

FRET Measurement of Nucleotide-Induced Conformational Changes of KF. Having established that tC is tolerated by KF, we examined the ability of this fluorescent base analogue to act as a spectroscopic reporter of conformational changes of the polymerase−DNA complex. The tC base was incorporated in the primer strand of duplex P1/T1 (Figure 4), immediately adjacent to the 3′ terminus, and the terminus was blocked with a 2′,3′-dideoxycytidine to prevent nucleotide incorporation when P1/T1 was mixed with KF and

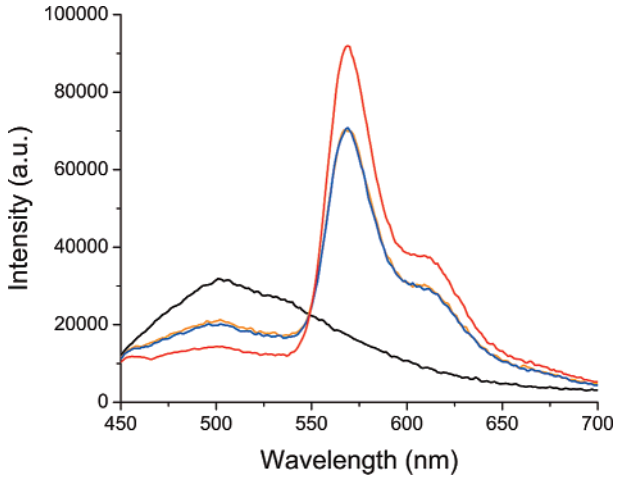

FIGURE 5: Fluorescence emission spectra demonstrating FRET between tC and A555. The tC base is located in the primer strand of primer/template P1/T1, adjacent to the 3′ terminus. The black spectrum shows the overall fluorescence of P1/T1 (500 nM) alone. The blue spectrum is for a binary complex of P1/T1 (500 nM) with A555-KF (1 μM). The A555 acceptor is attached to residue 751 within the O-helix of KF. The red spectrum is for a ternary complex of P1/T1 (500 nM), A555-KF (1 μM), and the correct nucleotide (dATP, 1 mM). The orange spectrum is for a ternary complex of P1/T1 (500 nM), A555-KF (1 μM), and the incorrect nucleotide (dCTP, 1 mM). All spectra were recorded with excitation at 393 nm and with 8 nm slits used for both excitation and emission.

nucleotide substrates. An Alexa-555 (A555) dye was attached to the unique cysteine residue (C751) of the S751C/C907S/D424A KF mutant. The C907S and D424A mutations remove the single native cysteine of KF and eliminate the 3′−5′ exonuclease activity of the enzyme, respectively. The introduced cysteine at position 751 is located in the O-helix of the fingers subdomain. Furey et al. (*41*) used the same mutant to label KF with a tetramethylrhodamine dye. From this point on, the mutations will not be explicitly referred to, although it should be understood that they are present in both the labeled and unlabeled KF derivatives. A555 was chosen to label KF for this study, because the absorption spectrum of the dye overlaps with the emission spectrum of tC (not shown), thereby creating a donor/acceptor pair for FRET measurements. The corresponding Förster distance for the tC/A555 pair is 49.0 Å, if a value of $^2/_3$ is assumed for the orientation factor. As noted above, cocrystal structures of open and closed ternary complexes of the KF homologue Klentaq1 reveal that the O-helix is rotated toward the DNA in the closed form (Figure 1). Accordingly, the donor−acceptor distance is expected to shorten during an open-to-closed conformational transition, leading to an increase in the FRET efficiency. The acceptor position should be particularly sensitive to the conformational change, since residue 751 is located at the outer end of the O-helix, which should maximize the change in donor−acceptor distance as the helix rotates toward the DNA.

The emission spectrum of free duplex P1/T1 is shown in Figure 5. Addition of a saturating amount of unlabeled KF to form a binary polymerase−DNA complex had no effect on the emission of tC (not shown). However, addition of A555-labeled KF led to a significant decrease in the donor peak at 505 nm, accompanied by the appearance of an intense acceptor peak at 570 nm (Figure 5). The observed acceptor emission originates entirely from FRET, since there is no direct excitation of A555 at the chosen excitation wavelength of 393 nm (data not shown). However, there is also a small contribution from the donor at 570 nm. The corresponding FRET efficiency (*E*), calculated from the decrease in donor emission at 505 nm, is 0.37. Subsequent addition of the correct nucleotide substrate (dATP, complementary to the templating base) led to a significant increase in FRET efficiency ($E = 0.55$), manifested as a decrease in donor emission and a corresponding increase in acceptor emission (Figure 5). In contrast, an incorrect nucleotide (dCTP) caused no appreciable change in either signal (Figure 5). Likewise, addition of either dGTP or dTTP (both incorrect) to the binary KF−DNA complex had no effect on the FRET efficiency (results not shown). Similar measurements of corresponding singly labeled complexes (donor-only or acceptor-only) confirmed that the nucleotides (either correct or incorrect) had no direct effect on the donor or acceptor emission (results not shown). Hence, this FRET system is monitoring a conformational change of the KF−DNA−dNTP ternary complex that occurs only in the presence of a correct incoming nucleotide.

The increase in FRET efficiency in the cognate ternary complex indicates a shortening of the donor−acceptor distance, consistent with the anticipated movement of the O-helix toward the DNA primer terminus (Figure 1). The donor−acceptor distances in the binary and ternary complexes, 53.6 and 47.4 Å, respectively, were estimated from the measured FRET efficiencies through the use of the Förster equation (*39*). These distances contain a significant contribution from the alkyl linker connecting the A555 acceptor to Cys751. Anisotropy data show that the local environment and rotational mobility of A555 are similar in binary and ternary complexes (results not shown), indicating that the linker adopts the same conformation in both cases. Hence, the linker contribution will cancel out when the difference in donor−acceptor distance between the binary and ternary complexes is evaluated. Accordingly, we estimate that the distance between the tC donor and A555 acceptor shortens by 6.2 Å during the nucleotide-induced conformational change, if a constant value of $^2/_3$ for the orientation factor in the binary and ternary complexes is assumed. This estimate is similar to the change in distance estimated from the cocrystal structures of Klentaq1 in open binary and closed ternary complexes (shortening of 8.5 Å). The latter value was obtained by measuring the distance between the −2 primer base (corresponding to the tC position) and the α-carbon atom of residue 656 of Klentaq1 (corresponding to the A555-labeled residue in KF) in the open binary and closed ternary complexes (*24*). In addition, we cannot exclude a small change in the orientation factor resulting from the ~40° rotation of the O-helix (*24*). Nevertheless, we conclude that the distance change inferred from the measured FRET efficiencies is consistent with an open-to-closed conformational transition of the fingers subdomain.

Effect of Nucleotides on DNA−KF Binding Affinity. To further probe the nature of the state induced by the correct nucleotide, we determined affinity constants for binding of KF to duplex P1/T1 in the presence and absence of nucleotides. Figure 6 presents the results of fluorescence anisotropy titrations in which increasing concentrations of unlabeled KF were added to a constant concentration of duplex P1/T1. Titrations were performed (1) in the absence

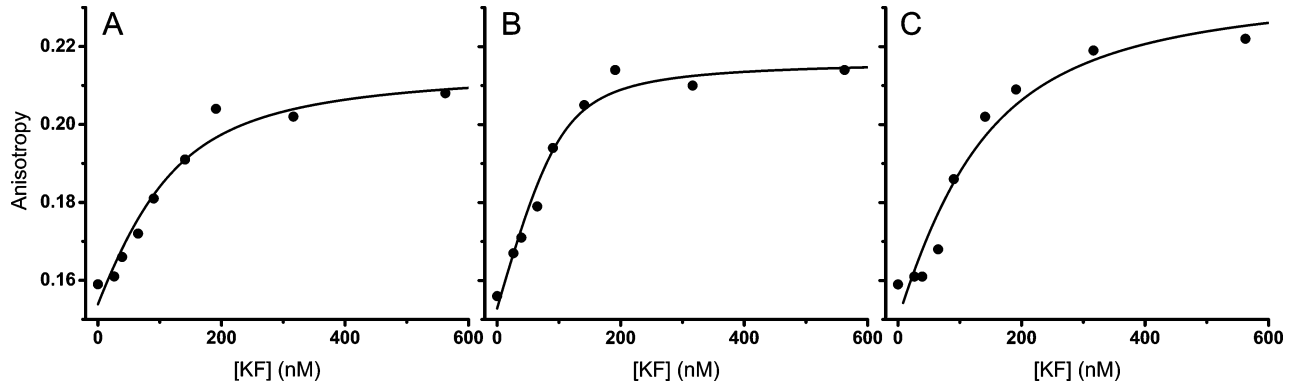

FIGURE 6: tC is a useful reporter of binding events in fluorescence anisotropy titration assays. The polarization anisotropy of tC increases upon addition of the indicated concentrations of unlabeled KF to primer/template P1/T1 (100 nM). Titrations were carried out (A) in the absence of nucleotides, (B) in the presence of the correct nucleotide dATP (1 mM), or (C) in the presence of the incorrect nucleotide dCTP (1 mM). The solid lines are best fits to a 1:1 association of KF with the primer/template. The corresponding K_d values are 52 ± 5 nM, 15 ± 2 nM, and 73 ± 7 nM, indicating that the correct nucleotide stabilizes the KF−DNA complex.

of any nucleotides, (2) in the presence of the correct nucleotide (dATP), or (3) in the presence of an incorrect nucleotide (dCTP). In all cases, the fluorescence anisotropy of tC increases from 0.16 in the free duplex to ~0.22 in the presence of saturating amounts of KF, reflecting the slower rotational diffusion of the duplex when the large KF protein was bound. The anisotropy profiles were fitted with a model of 1:1 association between the duplex and KF (*40*), yielding a dissociation constant (K_d) of 52 ± 5 nM for the binary complex. Interestingly, the DNA was bound more tightly by KF in the presence of the correct nucleotide (K_d = 15 ± 2 nM), consistent with the formation of a closed ternary complex with more extensive contacts between the enyzme and the DNA. In contrast, the presence of an incorrect nucleotide appeared to destabilize the binding of KF to the primer/template duplex (K_d = 73 ± 7 nM). The K_d value for the binary complex is larger than the values of 1−5 nM reported in previous studies of KF (*15*, *40*), suggesting that the tC probe interferes with binding to some extent. Nevertheless, the observed trends are in good agreement with previous KF−DNA binding measurements performed in the presence or absence of dNTPs (*42*).

Kinetics of Nucleotide-Induced Conformational Changes. Real-time kinetic FRET experiments were performed to measure the rate of the nucleotide-induced conformational transition of the KF−DNA complex. A binary complex was formed between primer/template P1/T1 and A555-KF, the complex was rapidly mixed with the correct nucleotide substrate dATP in a stopped-flow mixer, and the emission of both donor and acceptor was monitored over time. The donor emission was observed to decrease rapidly over time, while the acceptor emission increased correspondingly (Figure 7). Both transients were well described by a single-exponential curve, yielding rates of 7.7 ± 0.4 s^{-1} and 8.0 ± 0.3 s^{-1} for the donor and acceptor, respectively. The consistency of the donor and acceptor rates confirms that the observed emission changes are due to a time-dependent FRET process.

The amplitude of the FRET change observed in these kinetic measurements is in accord with the steady-state spectral measurements shown in Figure 5. The steady-state emission intensity of tC decreases by 26% between the binary and cognate ternary complexes, while the intensity of A555 increases by 29%. For comparison, the tC intensity decreases

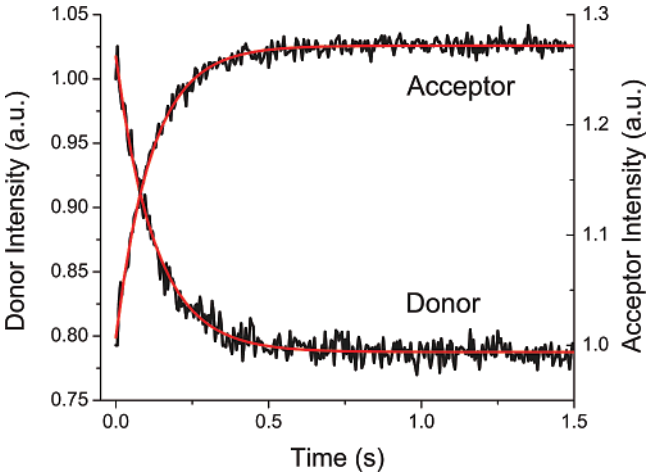

FIGURE 7: Kinetics of the nucleotide-induced conformational change of the KF−DNA complex measured in stopped-flow fluorescence experiments. A preformed binary complex of primer/template P1/T1 (500 nM) with A555-KF (1 μM) was rapidly mixed with a solution of the correct nucleotide dATP (1 mM) at a temperature of 20 °C, and the fluorescence intensity was measured as a function of time. The time-dependent decrease in tC donor emission and the corresponding increase in A555 acceptor emission are both well described by single-exponential functions (red lines), with rates of 7.7 ± 0.4 s^{-1} and 8.0 ± 0.3 s^{-1}, respectively.

by 24% over the time course shown in Figure 7, while the intensity of A555 increases by 27% over the same period. Hence, all of the expected signal changes were resolved in the stopped-flow experiments, indicating that any rapid (unresolved) processes must be of very small amplitude.

Kinetics of Nucleotide Incorporation. We measured the rate of correct nucleotide incorporation for comparison with the rate of the conformational change detected by FRET. The primer/template used for the incorporation reaction was identical to P1/T1, except that the primer was terminated with a normal 3′-OH group, and KF was labeled with A555, as before. The rate of dAMP incorporation was measured under pre-steady-state conditions on a rapid quench-flow instrument (Experimental Procedures). The rate of dAMP incorporation (7.6 ± 0.1 s^{-1}, Table 1) is very similar to the rate of the conformational change induced by dATP under the same experimental conditions (7.9 ± 0.2 s^{-1}, average of donor and acceptor rates). The agreement between these two rates indicates that the nucleotide-induced conformational

Table 1: Rates of dAMP Incorporation

primer/template[a]	enzyme[b]	k_{pol} (s^{-1})
5′AATCACGGCCC 3′TTAGTGCCGGGTGAAA	KF	52 ± 5
5′AATCACGGCCC 3′TTAGTGCCGGGTGAAA	A555-KF	23 ± 3
5′AATCACGGC^{t}CC 3′TTAGTGCCGGGTGAAA	KF	13 ± 3
5′AATCACGGC^{t}CC 3′TTAGTGCCGGGTGAAA	A555-KF	7.6 ± 0.1

[a] ^{t}C denotes the tC base. [b] KF denotes the S751C/C907S/D424A mutant Klenow fragment and A555-KF denotes the same mutant labeled with Alexa-555.

change is the rate-limiting step in the overall cycle of nucleotide incorporation.

We also measured the rate of dAMP incorporation using an unlabeled primer/template (tC replaced by C) and unlabeled KF. The resulting rate of 52 ± 5 s^{-1} (Table 1) is in agreement with values of 50 s^{-1} (*15*) and 46 s^{-1} (*43*) previously reported for wild-type KF, indicating that the C907S, S751C, and D424A mutations in our KF construct do not impair the activity of the enzyme. However, it is apparent that the presence of the tC and/or A555 probes in the doubly labeled KF−DNA system reduces the rate of nucleotide incorporation. To separately quantify the effect of each probe, we carried out rapid quench-flow experiments using the corresponding singly labeled KF-primer/template systems (Table 1). The results reveal that the presence of the tC probe within the primer/template reduces the rate of nucleotide incorporation ~4-fold, while the A555 dye attached to the protein causes a ~2-fold reduction in rate. The multiplicative effect of both modifications accounts for the overall reduction in activity observed for the doubly labeled system.

DISCUSSION

We have explored the potential of the fluorescent base analogue tC to serve as a reporter of polymerase−DNA interactions and conformational dynamics. Previous studies suggested that the tC base possesses favorable spectroscopic properties as a reporter of DNA−protein interactions (*29*). The chromophore has an absorption band at 393 nm and a broad emission band around 500 nm, allowing for selective excitation in the presence of unmodified nucleobases or aromatic amino acids within a bound protein. In addition, the fluorescence quantum yield of tC is relatively high (~0.2, *29*) and the fluorescence is not quenched when tC is incorporated in single- or double-stranded DNA, irrespective of the neighboring bases (*37*). In contrast, fluorescent base analogues such as 2-aminopurine (2AP) and 3-methylisoxanthopterin (3-MI) are strongly quenched in DNA (*31*−*36*). Here, we have also shown that the emission of tC is unaffected by binding of unlabeled KF to duplex P1/T1. Hence, the emission of tC is insensitive to both the local DNA and protein environment. These properties make tC an excellent choice as FRET donor, because any change in donor emission observed in the presence of an acceptor can be attributed to a change in FRET efficiency and donor−acceptor distance, rather than a change in local donor environment. Indeed, we observed a significant increase in FRET efficiency when a correct nucleotide substrate (dATP) was mixed with a binary complex of duplex P1/T1 and A555-labeled KF. The change in FRET efficiency was manifested as a decrease in tC donor emission and a corresponding increase in emission of the A555 acceptor. The anticorrelated nature of the donor and acceptor signals provides further confidence that the effects arise from a change in FRET efficiency. Moreover, addition of any of the three incorrect nucleotides to the binary complex did not cause any change in FRET efficiency. Hence, the FRET system described here is reporting a conformational change of the ternary polymerase−DNA−dNTP complex that occurs only in the presence of a correct nucleotide substrate.

Recently, several other fluorescence-based systems have been developed to monitor conformational changes of DNA polymerases during nucleotide binding and incorporation. Purohit et al. (*43*) and Bakhtina et al. (*44*) have used the fluorescent base analogue 2AP to probe conformational changes within the DNA substrate during nucleotide incorporation by KF. In both studies, the 2AP probe was located within the single-stranded region of the primer/template. Transient changes in 2AP emission were observed during the incorporation of a correct nucleotide into the DNA. However, the precise origin of these emission changes is uncertain. The fluorescence intensity of 2AP is influenced primarily by base-stacking interactions within the DNA (*33*). Hence, the emission transients could reflect a local conformational change within the DNA, such as base flipping, or a conformational transition of the polymerase, provided the latter is coupled to a change in base stacking. Tsai and Johnson (*45*) have also used a single fluorophore system to monitor nucleotide-induced conformational change of T7 DNA polymerase. In their system, an environmentally sensitive coumarin dye was attached to the fingers subdomain of the enzyme. The fluorescence intensity of the dye was observed to decrease upon addition of the correct nucleotide substrate to the binary polymerase−DNA complex, whereas the intensity actually increased in the presence of an incorrect nucleotide. Hence, the fluorescence quenching is reporting a process that is specific to the correct incoming nucleotide. However, it is unclear whether this process reflects a local conformational change in the vicinity of the dye or a global movement of the fingers subdomain.

In contrast to single-probe measurements, which are inherently ambiguous, a FRET system correlates the donor and acceptor emission intensity with a defined distance vector. By placing the tC donor close to the primer terminus and the A555 acceptor at the end of the mobile O-helix within the fingers subdomain, we have constructed a system that reports the physical movement of the O-helix toward the DNA. This system provides a direct readout of the open-to-closed conformational transition of the fingers, which occurs only in the presence of a correct incoming nucleotide substrate. Rothwell et al. (*46*) have also developed a FRET-based system to monitor nucleotide-induced conformational changes of Klentaq1 polymerase. In their system, an Alexa-488 donor dye was attached by a long linker to a base within the primer strand of the DNA and an Alexa-594 acceptor was attached to a cysteine residue within the fingers subdomain of Klentaq1. This system also reports the open-to-closed conformational transition of the fingers, although the donor position is not well-defined. In contrast, the tC donor in our FRET system stacks into the DNA helix just

like a normal base (*30*). Accordingly, the donor−acceptor distances measured with a tC donor are more readily related to the structure of the polymerase−DNA complex. Indeed, the shortening of the donor−acceptor distance observed during closure of the fingers is quantitatively consistent with the crystal structures of polymerase−DNA complexes in open and closed conformations.

The tC base can also be used to report the complexation of KF with primer/template DNA in quantitative binding titrations. Owing to the relatively long fluorescence lifetime of tC incorporated in DNA (*37*), the polarization anisotropy is sensitive to binding events that lead to slow rotational diffusion of the DNA. Indeed, binding of the large KF protein (∼68 kDa) to duplex P1/T1 can be monitored as a significant increase in the anisotropy of the tC emission. The K_d values for the polymerase−DNA complex were recovered under various conditions from analysis of the fluorescence anisotropy titrations. Interestingly, KF was bound more tightly to the primer/template in the presence of the correct nucleotide substrate, consistent with the formation of a closed ternary complex involving greater contacts between the enzyme and DNA.

In addition to favorable spectroscopic properties, tC is generally a good analogue of a natural cytosine base. We have shown that tC serves as a templating base to specifically direct the insertion of dGTP during a primer extension reaction. This is consistent with previous studies showing that tC base-pairs with G (*29*). Moreover, we have shown that a tC-terminated primer is extended only when the next correct nucleotide is supplied. Hence, the presence of tC at critical positions within the primer/template does not compromise the ability of KF to recognize and discriminate between correct and incorrect incoming nucleotides. However, while tC-containing primers can be extended by KF, the actual rate of nucleotide incorporation is reduced relative to natural primer/templates. Our results show that a tC base adjacent to the primer terminus reduces the rate of dAMP incorporation by ∼4-fold (Table 1). Similarly, the A555 probe attached to the fingers subdomain of KF causes a ∼2-fold reduction in the rate of nucleotide incorporation. These observations suggest that tC and A555 retard the conformational transition of the fingers subdomain or inhibit the chemical step of phosphoryl transfer. In fact, we found that the rate of the conformational transition ($7.9 \pm 0.2\ s^{-1}$, average of donor and acceptor rates) closely matched the rate of dAMP incorporation ($7.6 \pm 0.1\ s^{-1}$), indicating that the probes are primarily affecting the conformational change of the polymerase−DNA complex during nucleotide incorporation. Cocrystal structures of polymerase−DNA complexes reveal that the region of the primer/template around the primer 3′ terminus is in close contact with the protein, especially in the closed complex (*24*). Hence, it is not surprising that the bulky tC group and the A555 dye attached to the O-helix cause some slowing of the open-to-closed conformational transition. For the initial spectroscopic studies reported here, we deliberately incorporated tC close to the primer 3′ terminus and A555 within the O-helix, in order to maximize the FRET change that occurs during closure of the fingers subdomain. For future studies, tC can be incorporated further from the primer terminus and A555 can be located elsewhere in the fingers subdomain in order to mitigate the impact of the probes on the conformational transition.

The occurrence of an enzyme conformational change following correct nucleotide binding and preceding phosphoryl transfer may be a general property of many DNA polymerases (*23*). In Klentaq1 polymerase, addition of the next correct nucleotide induces an open-to-closed conformational transition of the fingers subdomain, which occurs rapidly in comparison to the rate of nucleotide incorporation (*46*). Similarly, the nucleotide-induced conformational change of T7 DNA polymerase is faster than the overall rate of nucleotide incorporation (*45*). In both these documented examples, conformational changes of the polymerase−DNA complex are not rate-limiting in the overall cycle of nucleotide incorporation. In contrast, we have shown that closure of the fingers subdomain and nucleotide incorporation proceed at the same rate, indicating that the conformational transition is the rate-limiting step for the doubly labeled KF−DNA system. Admittedly, the presence of the tC and A555 probes retards the rate of the conformational transition in our system. Nevertheless, our results establish that the conformational transition of the fingers subdomain *can* limit the overall rate of nucleotide incorporation. Of course, this does not imply that closure of the fingers is the rate-limiting step in nucleotide incorporation when unmodified KF acts on a normal DNA substrate. This issue can be directly addressed by use of the FRET system described here, with the tC and A555 probes positioned appropriately.

In summary, we have shown that the tC base analogue is an informative reporter of polymerase−DNA interactions and conformational dynamics, providing both thermodynamic and kinetic information. Since tC can be readily incorporated at any position in a primer/template and the A555 acceptor can be attached to a specific engineered cysteine residue within a selected region of the enzyme, there is considerable flexibility in donor/acceptor labeling. By combining such a labeling strategy with the FRET method described here, it will be possible to probe protein and/or DNA motions that are linked to the enzymatic function of DNA polymerase. We anticipate that the FRET system described here will be generally useful for mechanistic studies of DNA polymerases.

ACKNOWLEDGMENT

We thank Edwin Van der Schans for expert technical assistance and Goran Pljevaljcic for help in preparing the figures. We also thank Dr. Paul Schimmel (Scripps Research Institute) for the use of the Kintek rapid quench-flow instrument and Dr. Catherine Joyce (Yale University) for providing the plasmid encoding the D424A/C907S/S751C KF mutant.

REFERENCES

1. Kornberg, A., and Baker, T. A. (1992) *DNA Replication*, W. H. Freeman & Co.
2. Delarue, M., Poch, O., Tordo, N., Moras, D., and Argos, P. (1990) An attempt to unify the structure of polymerases, *Protein Eng. 3*, 461−467.
3. Fillee, J., Forterre, P., Sen-Lin, T., and Laurent, J. (2002) Evolution of DNA polymerase families: evidences for multiple gene exchange between cellular and viral proteins, *J. Mol. Evol. 54*, 763−773.
4. Ollis, D. L., Brick, P., Hamlin, R., Xuong, N. G., and Steitz, T. A. (1985) Structure of the large fragment of *Escherichia coli* DNA polymerase I complexed with dTMP, *Nature 313*, 762−766.

5. Korolev, S., Nayal, M., Barnes, W.M., Di Cera, E., and Waksman, G. (1995) Crystal structure of the large fragment of *Thermus aquaticus* DNA polymerase I at 2.5-Å resolution: Structural basis for thermostability, *Proc. Natl. Acad. Sci. U.S.A. 92*, 9264−9268.
6. Kim, Y., Eom, S. H., Wang, J., Lee, D. S., Suh, S. W., and Steitz, T. A. (1995) Crystal structure of *Thermus aquaticus* DNA polymerase, *Nature 376*, 612−616.
7. Kiefer, J. R., Mao, C., Hansen, C. J., Basehore, S. L., Hogrefe, H. H., Braman, J. C., and Beese, L. S. (1997) Crystal structure of a thermostable *Bacillus* DNA polymerase I large fragment at 2.1 Å resolution. *Structure 5*, 95−108.
8. Wang, J., Sattar, A. K. M. A., Wang, C. C., Karam, J. D., Konigsberg, W. H., and Steitz, T. A. (1997) Crystal structure of a pol α family replication DNA polymerase from bacteriophage RB69, *Cell 89*, 1087−1099.
9. Hopfner, K.-P., Eichinger, A., Engh, R. A., Laue, F., Ankenbauer, W., Huber, R., and Angerer, B. (1999) Crystal structure of a thermostable type B DNA polymerase from *Thermococcus gorgonarius*, *Proc. Natl. Acad. Sci. U.S.A. 96*, 3600−3605.
10. Sawaya, M. R., Pelletier, H., Kumar, A., Wilson, S. H., and Kraut, J. (1994) Crystal structure of rat DNA polymerase β: evidence for a common polymerase mechanism, *Science 246*, 1930−1935.
11. Zhou, B.-L., Pata, J. D., and Steitz, T. A. (2001) Crystal structure of a DinB lesion bypass DNA polymerase catalytic fragment reveals a classic polymerase catalytic domain, *Mol. Cell 8*, 427−437.
12. Trincao, J., Johnson, R. E., Escalante, C. R., Prakash, S., Prakash, L., and Aggarwal, A. K. (2001) Structure of the catalytic core of *S. cerevisiae* DNA polymerase η: Implications for translesion DNA synthesis, *Mol. Cell 8*, 417−426.
13. Uljon, S. N., Johnson, R. E., Edwards, T. A., Prakash, S., Prakash, L., and Aggarwal, A. K. (2004) Crystal structure of the catalytic core of human DNA polymerase kappa, *Structure 12*, 1395−1404.
14. Kohlstaedt, L. A., Wang, J., Friedman, J. M., Rice, P. A., and Steitz, T. A. (1992) Crystal structure at 3.5 Å resolution of HIV-1 reverse transcriptase complexes with an inhibitor, *Science 256*, 1783−1790.
15. Kuchta, R. D., Mizrahi, P. A., Benkovic, P. A., Johnson, K. A., and Benkovic, S. J. (1987) Kinetic mechanism of DNA polymerase I (Klenow fragment), *Biochemistry 26*, 8410−8417.
16. Wong, I., Patel, S. S., and Johnson, K. A. (1991) An induced fit kinetic mechanism for DNA polymerase fidelity: direct measurement by single turnover kinetics, *Biochemistry 30*, 526−537.
17. Steitz, T. A. (1999) DNA polymerases: Structural diversity and common mechanisms, *J. Biol. Chem. 274*, 17395−17398.
18. Capson, T. L., Peliska, J. A., Kaboord, B. F., Frey, M. W., Lively, C., Dahlberg and Benkovic, S. J. (1992) Kinetic characterization of the polymerase and exonuclease activities of the gene 43 protein of bacteriophage T4, *Biochemistry 31*, 10984−10994.
19. Ahn, J., Werneburg, B. G., and Tsai, M. D. (1997) DNA polymerase β: structure-fidelity relationships from pre-steady-state kinetic analyses of all possible correct and incorrect base pairs for wild-type and R283A mutant, *Biochemistry 36*, 1100−1107.
20. Washington, M. T., Prakash, L., and Prakash, S. (2001) Yeast DNA polymerase η utilizes an induced-fit mechanism of nucleotide incorporation, *Cell 107*, 917−927.
21. Fiala, K. A., and Suo, Z. (2004) Mechanism of DNA polymerization catalyzed by *Sulfolobus solfataricus* P2 DNA polymerase IV, *Biochemistry, 43*, 2116−2125.
22. Fiala, K.A., and Suo, Z. (2004) Pre-steady-state kinetic studies of the fidelity of *Sulfolobus solfataricus* P2 DNA polymerase IV, *Biochemistry 43*, 2106−2115.
23. Joyce, C. M., and Benkovic, S. J. (2004) DNA polymerase fidelity: Kinetics, structure and checkpoints, *Biochemistry 43*, 14317−14324.
24. Li, Y., Kong, Y., Korolev, S., and Waksman, G. (1998) Crystal structures of open and closed forms of binary and ternary complexes of the large fragment of *Thermus aquaticus* DNA polymerase I: Structural basis for nucleotide incorporation, *EMBO J. 17*, 7514−7525.
25. Franklin, M. C., Wang, J., and Steitz, T. A. (2001) Structure of the replicating complex of a pol α family DNA polymerase, *Cell 105*, 657−667.
26. Huang, H., Chopra, R., Verdine, G. L., and Harrison, S. C. (1998) Structure of a covalently trapped catalytic complex of HIV-1 reverse transcriptase: Implications for drug resistance, *Science 282*, 1669−1675.
27. Yang, L., Beard, W. A., Wilson, S. H., Broyde, S., and Schlik, T. (2002) Polymerase β simulations suggest that Arg258 rotation is a slow step rather than large subdomain motions per se. *J. Mol. Biol. 317*, 651−671.
28. Zhong, X., Patel, S. S., Werneburg, B. G., and Tsai, M. D. (1997) DNA polymerase β: multiple conformational changes in the mechanism of catalysis, *Biochemistry 36*, 11891−11900.
29. Wilhelmsson, M., Holmen, A., Lincoln, P., Nielsen, P. E., and Norden, B. A. (2001) highly fluorescent DNA base analogue that forms Watson-Crick base pairs with guanine, *J. Am. Chem. Soc. 123*, 2434−2435.
30. Engman, K. C., Sandin, P., Osborne, S., Brown, T., Billeter, M., Lincoln, P., Norden, B., Albinsson, B., and Wilhelmsson, M. L. (2004) DNA adopts normal B-form upon incorporation of highly fluorescent DNA base analogue tC: NMR structure and UV-Vis spectroscopy characterization, *Nucleic Acids Res. 32*, 5087−95.
31. Nordlund, T. M., Andersson, S., Nilsson, L., and Rigler, R. R. (1989) Structure and dynamics of a fluorescent DNA oligomer containing the *Eco*RI reognition sequence: Fluorescence, molecular dynamics and NMR studies, *Biochemistry 28*, 9095−9103.
32. Guest, C. R., Hochstrasser, R. A., Sowers, L. C., and Millar, D. P. (1991) Dynamics of mismatched base pairs in DNA. *Biochemistry 30*, 3271−3279.
33. Rachovsky, E. L., Osman, R., and Ross, J. B. A. (2001) Probing structure and dynamics of DNA with 2-aminopurine: Effects of local environment on fluorescence, *Biochemistry 40*, 946−956.
34. Driscoll, S. L., Hawkins, M. E., Balis, F. M., Pfleiderer, W., and Laws, W. R. (1997) Fluorescence properties of a new guanosine analog incorporated into small oligonucleotides, *Biophys. J. 73*, 3277−3286.
35. Wu, P., Nordlund, T. M., Gildea, B., and McLaughlin, L. W. (1990) Base stacking and unstacking as determined from a DNA decamer containing a fluorescent base, *Biochemistry 29*, 6508−6514.
36. Singleton, S. F., Shan, F., Kanan, M. W., McIntosh, C. M., Sterman, C. J., Helm, J. S., and Webb, K. J. (2001) Facile synthesis of a fluorescent deoxycytidine analogue suitable for probing the RecA nucleoprotein filament, *Org. Lett. 3*, 3919−3922.
37. Sandin, P., Wilhelmsson, M. L., Lincoln, P, Powers, V. E., Brown, T., and Albinsson, B. (2005) Fluorescent properties of base analogue tC upon incorporation into DNA—negligible influence of neighbouring bases on fluorescence quantum yield, *Nucleic Acids Res. 33*, 5019−5025.
38. Joyce, C. M., and V. Derbyshire, V. (1995) Purification of *Escherichia coli* DNA polymerase I and Klenow fragment, *Methods Enzymol. 262*, 3−13.
39. Lakowicz, J. R. (1999) *Principles of Fluorescence Spectroscopy*, 2nd ed., Chapter 13, Kluwer Academic/Plenum Publishers.
40. Bailey, M. F., Van der Schans, E. J. C., and Millar, D. P. (2004) Thermodynamic dissection of the polymerizing and editing modes of a DNA polymerase, *J. Mol. Biol. 336*, 673−693.
41. Furey, W. S., Joyce, C. M., Osborne, M. A., Klenerman, D., Peliska, J. A., and Balasubramanian, S. (1998) Use of fluorescence resonance energy transfer to investigate the conformation of DNA substrates bound to the Klenow fragment, *Biochemistry 37*, 2979−2990.
42. Dzantiev, L., and Romano, L. J. (1999) Interaction of *Escherichia coli* DNA polymerase I (Klenow fragment) with primer-templates containing *N*-acetyl-2-aminofluorene or *N*-2-aminofluorene adducts in the active site, *J. Biol. Chem. 274* 3279−3284.
43. Purohit, V. Grindley, N. D. F., and Joyce, C. M. (2003) Use of 2-aminopurine to examine conformational changes during nucleotide incorporation by DNA polymerase I (Klenow fragment), *Biochemistry 42*, 10200−10211.
44. Bakhtina, M., Roettger, M. P., Kumar, S., and Tsai, M.-D. (2007) A unified kinetic mechanism applicable to multiple DNA polymerases, *Biochemistry 46*, 5463−5472.
45. Tsai, C.-H., and Johnson, K. A. (2006) A new paradigm for DNA polymerase specificity, *Biochemistry 45*, 9675−9687.
46. Rothwell, P. J., Mitaksov, V., and Waksman, G. (2005) Motions of the fingers subdomain of Klentaq1 are fast and not rate-limiting: Implications for the molecular basis of fidelity in DNA polymerases, *Mol. Cell 19*, 345−355.

BI700755M